Matrix isolation and computational study of the photochemistry of *p*-azidoaniline†

Elena A. Pritchina,[a] Nina P. Gritsan*[a] and Thomas Bally*[b]

Received 5th August 2005, Accepted 11th November 2005
First published as an Advance Article on the web 15th December 2005
DOI: 10.1039/b511229j

The photochemistry of *p*-azidoaniline was studied in argon matrices in the absence and presence of oxygen. With the help of quantum chemical calculations we were able to characterize the triplet *p*-aminophenylnitrene as well as the *cis*- and *trans*-*p*-aminophenylnitroso oxides. It was found that the latter two isomers can be interconverted by selective irradiation and that they are ultimately converted into *p*-nitroaniline. Although restricted wavefunctions of the nitroso oxides are unstable, CASSCF calculations turned up no evidence for the claimed diradical character of these compounds. Also we found no evidence for dioxaziridines as intermediates of the conversion of the nitroso oxides to *p*-nitroaniline.

1 Introduction

Great progress has been made in understanding the photochemistry of aryl azides over the past few years.[1,2] Singlet phenylnitrene and a series of its simple derivatives have been detected directly and the effects of substituents on the spectra and the decay kinetics of singlet aryl nitrenes have been examined systematically.[2] Thereby it was found that groups which act as strong π donors dramatically accelerate the rate of intersystem crossing. This could be the reason why photolysis of *p*-azidoaniline (**1**) and *p*-azidodimethylaniline, unlike that of phenyl azide and most of its derivatives, gives only products of triplet nitrene reactions.[3,4] For instance, in the presence of oxygen at ambient temperature *p*-nitroaniline (**2**) and *p*-nitrosoaniline (**3**) are formed in quantitative yield upon photolysis of **1** (Scheme 1).[3,5]

Since the early seventies it has been known that triplet arylnitrenes react with oxygen by formation of adducts.[5–9]

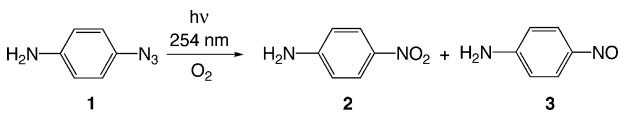

Scheme 1

In an early study on 1,4-diazidobenzene, two types of adducts (diamagnetic and paramagnetic) were detected in glassy matrices.[6] It was proposed that the diamagnetic adduct is an arylnitroso oxide, R–N═O^+–O^-, and the paramagnetic species is a "spin isomer" thereof, the triplet aryliminodioxy diradical, R–N–O•–O•.[6,10] Although subsequent studies did not confirm the formation of triplet adducts of arylnitrenes with oxygen,[3,5,7,8] speculations about the occurrence of aryliminodioxy diradicals in the photooxidation of aryl azides continue to surface occasionally in the literature.[11]

This paper is devoted to a comprehensive experimental and computational study of the reactions of triplet arylnitrenes with oxygen in order to unambiguously identify the resulting adducts by their experimentally observed spectra, and to understand their properties. It should be noted that the earlier assignments of a strong near-UV absorption to arylnitroso oxides[3,5,7–9] were never supported by calculations. *p*-Azidoaniline was used in our matrix isolation study because, as noted above, it gives exclusively products of triplet nitrene reactions in solution, and we thought that this would also simplify the photochemistry in Ar matrices. In addition, the reaction of triplet *p*-aminophenylnitrene (**4**) with oxygen in solution and in glassy matrices has previously been studied.[5]

2 Experimental and computational details

p-Azidoaniline (**1**) was synthesized following the published procedure.[12]

Spectroscopy in argon matrices[13]

A few ground crystals of **1** were placed in a U-tube attached to the inlet system of the cryostat. During deposition the temperature of the U-tube was kept at about 0 °C. To study the photochemistry of **1** in the absence of oxygen, a mixture of argon (Carbagas, 99.995%) with 10% nitrogen (Carbagas, 99.995%) flowed through the U-tube, carrying along appropriate quantities of **1** to form, upon freezing of the gaseous mixture on a CsI window (UV transparent quality, Korth

[a] *Institute of Chemical Kinetics and Combustion, Siberian Branch of Russian Academy of Sciences and Novosibirsk State University, 630090 Novosibirsk, Russia. E-mail: gritsan@kinetics.nsc.ru*
[b] *Department of Chemistry, University of Fribourg, ch du Musée 9, CH-1700 Fribourg, Switzerland. E-mail: Thomas.Bally@unifr.ch*

† Electronic supplementary information (ESI) available: Cartesian coordinates of all stationary points located in this study and details of the CASSCF/CASPT2 calculations (text file). Calculated spectrum of nitrene **4** at its C_s geometry (Fig. S1 and Table S1); IR spectra of **8** calculated by UB3LYP and RB3LYP (Fig. S3); calculated optical spectra of **7** and **8** at the B3LYP geometries (Tables S5 and S8); calculations of the thermodynamics of the formation of adducts between triplet nitrene and molecular oxygen and their further rearrangements in both spin states by the B3LYP/6-311G(d,p), G2M(CC5) and CBS-QB3 levels of theory (Figs. S4–S5 and Tables S10–S12); calculated IR and EA spectra of the cyclic dioxaziridine (Fig. S6 and Table S13) (pdf file). See DOI: 10.1039/b511229j

Kristalle GmbH) maintained at *ca*. 20 K, a matrix giving reasonable optical densities of azide and the products of its photolysis. After deposition the matrix was cooled to the lowest limit attainable by the closed-cycle cryostat (*ca*. 12 K). **1** was bleached with a low-pressure mercury lamp (254 nm). Subsequent irradiations were effected using a medium-pressure Hg/Xe lamp and appropriate interference and cutoff filters, or a monochromator.

In order to study the reaction of triplet *p*-aminophenylnitrene (**4**) with oxygen, a mixture of 86% argon, 10% nitrogen and 4% oxygen was led through the U-tube containing **1** and condensed on the CsI window. After photolysis of the resulting matrix at 254 nm it was heated to 20 K and kept at this temperature for about 5 min. Then, the sample was annealed at 25 and 30 K for 5 min each after which it was cooled back down to 12 K.

Electronic absorption spectra were obtained on a Perkin-Elmer Lambda 900 spectrometer (200–1000 nm). IR spectra were measured on a Bomem DA3 interferometer (4000–500 cm^{-1}) with an MCT detector.

Quantum chemical calculations

The geometries and harmonic vibrational frequencies of *p*-azidoaniline (**1**), *p*-aminophenylnitrene (**4**) and its isomers and adducts with oxygen were calculated at the B3LYP[14,15] and/or CASSCF[16] levels of theory with the 6-31G(d) basis set, using the GAUSSIAN-98[17] and MOLCAS[18] suites of programs. All equilibrium structures were ascertained to be minima on the potential energy surfaces and the stability of the SCF solutions was tested. The harmonic frequencies calculated by B3LYP/6-31G(d) were scaled by the recommended factor of 0.9614[19] for their use in assigning the experimental IR spectra.

Excited state energies were calculated at the B3LYP/6-31G(d) and CASSCF/6-31G(d) geometries by the CASSCF/CASPT2 procedure[20] with the ANO-S basis set of Pierloot *et al.*[21] using the MOLCAS program.[18] In order to arrive at a satisfactory description of all excited states at the CASPT2 level (*i.e*. remove intruder states) it was necessary to resort to the level-shifting technique,[22] whereby it was carefully ascertained that no artifacts are introduced. The active spaces used in these calculations are described in the text and depicted in Figs. 3 and 10. To predict the electronic absorption spectra of the keteneimine and the azirine the time-dependent (TD) DFT method[23] (as implemented in the Gaussian program[24]) with the B3LYP combination of exchange[14] and correlation functionals[14,15] was used with the 6-31+G(d) basis set.

The enthalpy changes for the reactions of triplet phenylnitrene and its *p*-amino derivative with oxygen were evaluated at the CBS-QB3,[25] G2M(CC5MP2)[26] and B3LYP/6-311G(d,p) level of theory.

3 Results and discussion

Photolysis of *p*-azidoaniline in an Ar matrix

Before studying the reaction of triplet *p*-aminophenylnitrene (**4**) with oxygen, we photolyzed **1** in an Ar matrix in the absence of oxygen. After 3 min of 254 nm photolysis the electronic absorption spectrum of **1** (dashed line, spectrum *a* in Fig. 1) was replaced by a new band with a maximum at 287 nm and two structured band systems in the near UV (305–340 nm) and visible (380–480 nm) regions (solid line, spectrum *b* in Fig. 1). Under the same conditions, the IR bands of **1**, in particular the strong 2116 cm^{-1} N_3-stretching vibration, disappeared completely. Therefore we assigned the newly formed UV/Vis spectrum to the triplet *p*-aminophenylnitrene **4**. The black bars in Fig. 1 show that the excited state energies and relative transition moments of **4** calculated by the CASSCF/CASPT2 procedure (see below) are in very good agreement with the experimental spectrum. These calculations suggest *e.g*. that the first band system in the experimental spectrum of **4** encompasses weakly allowed electronic transitions to *two* electronic states. Similar to the cases of the iso-π-electronic benzyl radical[27] and phenylcarbene molecules,[28] pronounced vibronic mixing between these two states makes that the vibrational structure of the first band system of **4** cannot be rationalized on the basis of an adiabatic Franck–Condon model.

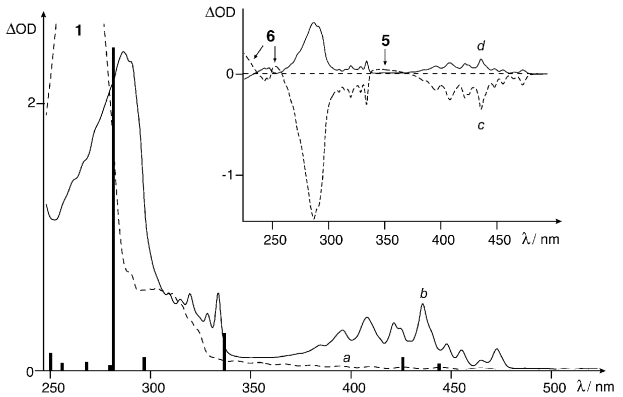

Fig. 1 Electronic absorption spectrum for the bleaching of *p*-azidoaniline (**1**, spectrum *a*, dashed line) in an Ar matrix at 12 K at 254 nm for 3 min (spectrum *b*, solid line). The calculated positions and relative oscillator strengths of the electronic transitions of nitrene **4** are depicted as black bars. Inset: changes upon 16 min irradiation of **4** at > 375 nm (dashed line, spectrum *c*) and upon subsequent irradiation for 5 min at 313 nm (solid line, spectrum *d*).

In the IR spectrum, the bands of **1** give way to a set of new peaks on 254 nm photolysis (Fig. 2, spectrum *a*). Most of these new peaks correlate well with the IR spectrum calculated for **4** (trace *b*). However, some of less intense peaks which are marked with asterisks, for instance the characteristic 1879 cm^{-1} line, continue to grow on subsequent short irradiation of the sample at > 375 nm which leads to the bleaching of **4** (spectrum *d*). These peaks coincide well with the spectrum calculated for keteneimine **5** (Fig. 2, trace *c* and Scheme 2), except for the two strong peaks predicted to occur around 1600 cm^{-1} which are probably masked in the difference spectrum by the decreasing peaks of **4** in that region.

The fact that keteneimine **5** is not formed upon irradiation of azide **1** in solution at ambient temperature, but is produced upon photolysis of the triplet nitrene **4** at 12 K indicates that its formation during the decomposition of the azide in Ar is probably due to secondary photolysis of **4**, also because the **5**/**4** ratio increases with the irradiation time (after complete photo-decomposition of the azide **1**, the triplet nitrene **4**

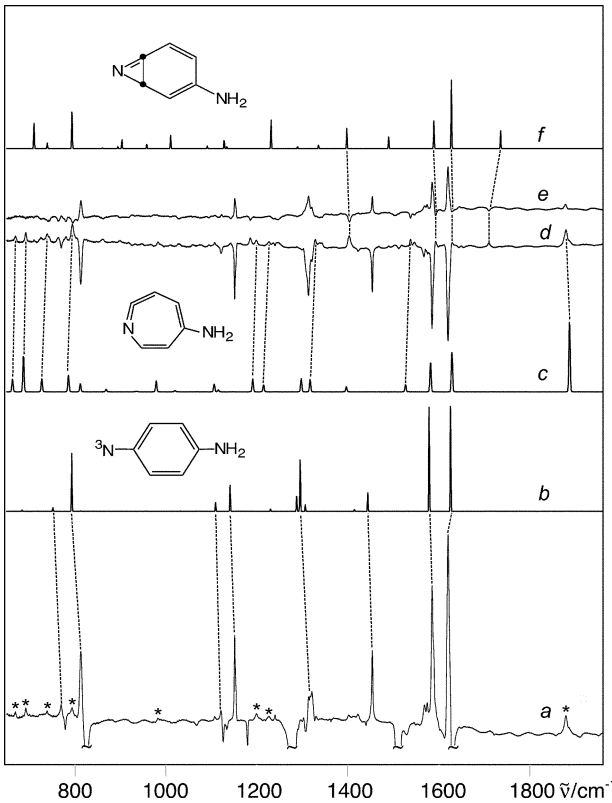

Fig. 2 Difference IR spectrum for the bleaching of *p*-azidoaniline (**1**) in an Ar matrix at 12 K to 254 nm for 3 min (spectrum *a*, the downward pointing peaks of **1** are clipped). Changes upon 16 min irradiation of **4** at >375 nm (spectrum *d*) and upon subsequent irradiation for 5 min at 313 nm (spectrum *e*). The traces *b*, *c*, and *f* show the IR-spectra of triplet *p*-aminophenylnitrene (**4**), keteneimine (**5**) and azirine (**6**), respectively, calculated by B3LYP and scaled by 0.9614.

accounts for only *ca.* 80% of the product according to the IR band intensities).

However, the bleaching of nitrene **4** did not only give rise to **5** but also to a product which has weak IR-bands at 795, 1185, 1403, 1503, and 1710 cm^{-1} that are in turn bleached on subsequent irradiation of the sample at 313 nm (spectrum *e* in Fig. 2). According to the literature[29,30] naphtho- and benzoazirines have characteristic C=N–stretching vibrations at 1680–1730 cm^{-1}. Therefore, we are tempted to assign the peak at 1710 cm^{-1} to the amino-substituted benzazirine **6** although the other peaks in the calculated spectrum of **6** (Fig. 2, spectrum *f* and Scheme 2) are not clearly observed in the difference spectra *d* and *e*, perhaps due to their coincidence with stronger bands of **4** and/or **5**.

In the UV/Vis difference spectra for the >375 nm bleaching of **4** and its partial re-formation on 313 nm irradiation (inset to Fig. 1, spectra *c* and *d*), the keteneimine **5** manifests itself weakly by its characteristic broad absorption around 350 nm,[1,2] whereas **6** seems to absorb only below 260 nm. Note that a benzazirine analogous to **6** was not detected upon photolysis of phenyl azide in an Ar matrix.[31,32]

As seen in Fig. 1, the electronic absorption (EA) spectrum of triplet nitrene **4** is well reproduced by CASSCF/CASPT2

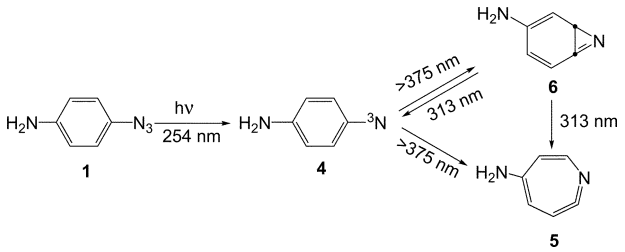

Scheme 2

calculations. The same procedure has been used previously for the assignment of the EA spectrum of parent triplet phenylnitrene (^{3}**PN**),[33] which permits us to analyze the influence of the amino group on the EA spectrum of triplet phenylnitrene. Due to pyramidalization of the NH_2 group **4** has only C_s-symmetry, whereas ^{3}**PN** is planar and has C_{2v}-symmetry. For the purpose of comparing the electronic transitions of the two nitrenes, we therefore ran additional calculations, where **4** was constrained to be planar (C_{2v}-symmetry). The active space used in these calculations consists of the twelve MOs depicted in Fig. 3.

As the calculated spectra of nitrene **4** at its C_{2v} and C_s geometry do not differ much (*cf.* ESI, Fig. S1 and Table S1),† we present only the data for the planar form (Table 1, Fig. 3). Note that the experimental spectrum could be slightly contaminated in the region of 350–400 nm by the weak absorption of keteneimine **5**.[34]

As in the benzyl radical and in related iso-π-electronic systems, the main absorption bands in phenylnitrenes come in pairs of disparate intensity that represent transitions to the positive and negative combinations of two π electronic configurations.[28] Thus, the first and the third band in the spectrum of **4** (with origins at 473 and 333 nm) involve excitations from the benzene-like $1a_2$-MO to the benzylic $4b_1$ SOMO and from there to the benzene-like $2a_2$ LUMO to form a pair of $^3B_1$ states (solid arrows in Fig. 3), whereas the second band with λ_{max} = 435 nm and the intense UV band peaking at 290 nm are due to excitations from the doubly occupied $3b_1$ MO to the π-SOMO and from there to the virtual $5b_1$ MO, giving rise to a pair of $^3A_2$ states (dashed arrows in Fig. 3).

On going from ^{3}**PN**[33] to **4** the first band undergoes almost no shift but gains an order of magnitude in intensity according to CASSCF, whereas the "electronically related" third band, which nearly coincides with the intense UV band in ^{3}**PN**, is shifted by about 30 nm in **4** where it is now clearly separated in the spectrum. In contrast, the second band which peaks at *ca.* 375 nm in ^{3}**PN**, is shifted to 435 nm in **4** (while its intensity changes very little), whereas the intense UV-peak undergoes only a small blue-shift of about 10 nm. Note that our present calculations, which are in good quantitative accord with the experimental spectrum of **4** and nicely bear out its resemblance to that of the benzyl radical,[28] predict that the intense UV band is mainly due to the $1\,^3A_2 \rightarrow 3\,^3A_2$ excitation, in contrast to the assignment of the intense UV band of parent ^{3}**PN** to the $1\,^3A_2 \rightarrow 2\,^3B_1$ and/or the $1\,^3A_2 \rightarrow 3\,^3B_1$ transitions.[33] We plan to reexamine this assignment in a comparative study of the electronic structure of different phenylnitrenes.

As in the related case of triplet phenylcarbene,[28] excitations to or from the σ-SOMO ($9b_2$) of ^{3}**PN** or **4** do not manifest

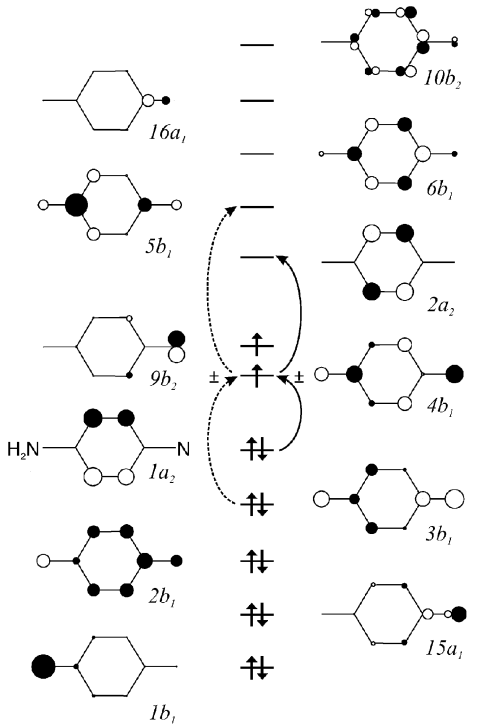

Fig. 3 Active space used in the CASSCF/CASPT2 calculations of the electronic transitions of nitrene **4** (*cf.* Table 1). The excitations that contribute mainly to the first few optical transitions, leading to the lowest two excited states of B_1 and A_2 symmetry, respectively, are marked with arrows (for discussion see text).

themselves palpably in the absorption spectrum because excitations from π-MOs into this SOMO are either dipole forbidden ($1\ ^3A_2 \rightarrow 1\ ^3A_1$) or only very weakly allowed ($1\ ^3A_2 \rightarrow 3\ ^3B_2$). In contrast, excitations from the sp-lone pair on the N atom ($15a_1$) to the σ-SOMO ($1\ ^3A_2 \rightarrow 3\ ^3B_1$) or to the π-SOMO ($1\ ^3A_2 \rightarrow 3\ ^3B_2$) give rise to transitions that might contribute to the intense UV band of **4** or other phenylnitrenes.[35] Unfortunately we cannot verify this prediction experimentally because the intense $1\ ^3A_2 \rightarrow 3\ ^3A_2$ transition masks weaker bands in its vicinity.

Photolysis of *p*-azidoaniline in an Ar matrix doped with oxygen

Photolysis of **1** in an Ar matrix containing 4% oxygen leads to the same products as before, *i.e.* nitrene **4** and keteneimine **5** (Fig. 4, spectrum *a*). Subsequent annealing of the matrix at 30 K allows for slow diffusion of O_2 and its reaction with **4**, which manifests itself in the formation of an intense new absorption in the visible region (Fig. 4, spectrum *b*, λ_{max} = 445 nm). Simultaneously, the IR bands of **4** decrease and give way to a set of new peaks (upward pointing peaks in spectrum *a* of Fig. 5). Note that the visible band of the adduct between **4** and O_2 formed at 95 K in a glassy THF–toluene (1 : 1) matrix is significantly red-shifted (λ_{max} = 495 nm), but the maximum of this band shifts also from 440 nm in hexane to 470 nm in toluene at 285 K.[5]

Subsequent irradiation of the sample for 5 min at the long wavelength tail of the visible band (> 515 nm) leads to its disappearance and the formation of the UV band (Fig. 4, spectrum *c*, λ_{max} = 326 nm) and the IR peaks of *p*-nitroaniline (**2**) (Fig. 5, positive peaks marked by asterisks in spectrum *b*).

Our earlier EPR and EA experiments[5] had shown that the adduct of **4** with oxygen formed in glassy matrices at 77 K has a singlet ground state and exists in two forms which could be interconverted photochemically. At the time we had tentatively proposed that the two forms are the *cis*- (**7**) and the *trans*-isomer (**8**) of *p*-aminophenylnitroso oxide.[5]

The same two species were formed in the reaction of triplet nitrene **4** with oxygen in an Ar matrix at 30 K. One of them disappeared upon irradiation for 30 s (λ > 515 nm) and was converted to *p*-nitroaniline **2** (Fig. 6 and 7, upward pointing peaks in spectrum *a*). This intermediate is characterized by an intense absorption in the visible region (Fig. 6, spectrum *a*, λ_{max} = 460 nm) and a set of peaks in IR (Fig. 7, downward pointing peaks in spectrum *a*).[36] After photolysis of the sample at > 515 nm for another 5 min, the second intermediate is also converted to **2**. This species has a similarly intense, but blue-shifted band (Fig. 6, spectrum *b*, λ_{max} = 425 nm) and a number of associated IR-peaks (Fig. 7, downward pointing peaks in spectrum *b*).[37]

When the samples were photolyzed through a monochromator we observed a photochemical interconversion of the two species (along with the formation of some **2**): on 30 min of

Table 1 Vertical excitation energies of triplet *p*-aminophenylnitrene **4** calculated by the CASPT2 method[a]

State	ΔE_{CASSCF}/eV	ΔE_{CASPT2}/eV	Reference weight[b]	λ/nm	*f*[c]	Major configurations[d]
$1\ ^3A_2$	0.00	0.00	0.78	—	—	80% ground config.
$1\ ^3B_1$	3.27	2.80	0.76	442	4.4×10^{-3}	30% $1a_2 \rightarrow 4b_1$ − 42% $4b_1 \rightarrow 2a_2$
$2\ ^3A_2$	3.26	2.91	0.77	426	1.3×10^{-2}	47% $3b_1 \rightarrow 4b_1$ + 30% $4b_1 \rightarrow 5b_1$
$2\ ^3B_1$	5.47	3.66	0.74	338	3.8×10^{-2}	37% $1a_2 \rightarrow 4b_1$ + 28% $4b_1 \rightarrow 2a_2$
$1\ ^3A_1$	3.86	3.77	0.75	329	0.0	85% $3b_1 \rightarrow 9b_2$
$3\ ^3B_1$	4.64	4.17	0.76	297	1.4×10^{-2}	80% $15a_1 \rightarrow 9b_2$
$3\ ^3A_2$	6.34	4.42	0.74	281	3.5×10^{-1}	24% $3b_1 \rightarrow 4b_1$ − 38%: $4b_1 \rightarrow 5b_1$
$1\ ^3B_2$	5.42	4.44	0.71	280	2.1×10^{-3}	64% $4b_1 \rightarrow 16a_1$
$4\ ^3A_2$	4.63	4.44	0.77	279	5.7×10^{-3}	59% [$9b_2 \rightarrow 2a_2$ (β) + $1a_2 \rightarrow 9b_2$ (α)]
$2\ ^3B_2$	5.84	4.63	0.72	268	9.0×10^{-3}	81% $15a_1 \rightarrow 4b_1$
$3\ ^3B_2$	5.97	4.69	0.73	264	1.4×10^{-5}	58% $1a_2 \rightarrow 9b_2$

[a] Based on a CASSCF(12,12)/ANO-S wave function at the CASSCF(8,8)/6-31G(d) geometry; A_1 and B_2 states were calculated with no level shift, B_1 states-with a level shift of 0.1 h, A_2 states-with a level shift of 0.2 h. The results for higher excited states are listed in the ESI.† [b] Weight of the zero-order CASSCF in the CASPT2 wave function. [c] Oscillator strength for electronic transition. [d] Electron excitations within the active space of orbitals depicted in Fig. 3

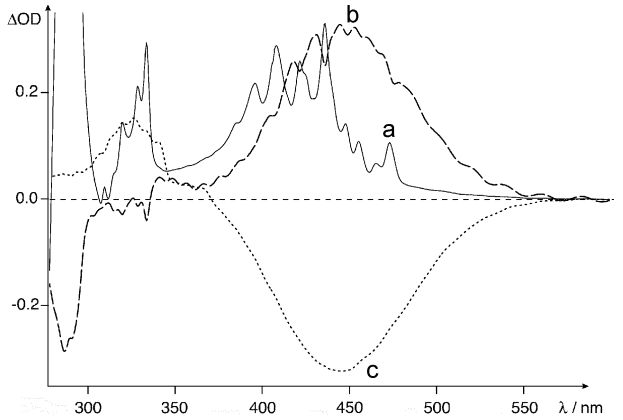

Fig. 4 Difference EA-spectrum for the formation of nitrene **4** (contaminated by some keteneimine **5**) in an Ar matrix containing 4% oxygen at 12 K (spectrum *a*, solid line). Change after annealing the sample at 30 K (dashed spectrum *b*). Changes upon 5 min irradiation at >515 nm (dotted spectrum *c*).

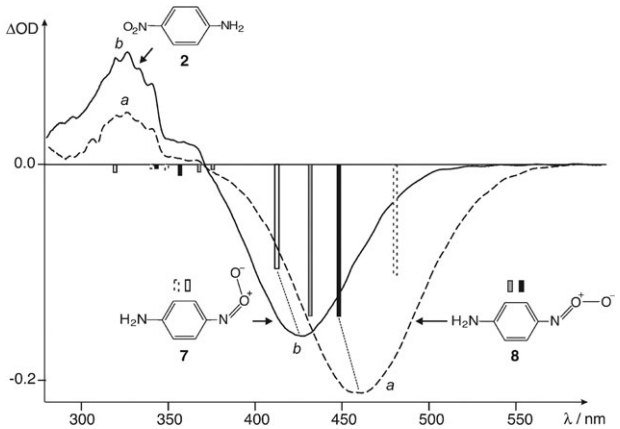

Fig. 6 Difference EA spectra of the adducts of nitrene **4** with oxygen produced by bleaching in an Ar matrix at 12 K to >515 nm for 30 s (spectrum *a*, dashed line) and for 5 min (spectrum *b*, solid line). The bars indicate the positions and relative oscillator strengths of the electronic transitions of the nitroso oxides **8** (black and gray bars) and **7** (open and dashed bars), calculated by the CASSCF/CASPT2 method at the geometries optimized by the CASSCF (solid and open bars) and B3LYP/6-31G(d) (grey and dashed bars).

irradiation at 515 nm the carrier of the 460 nm band was partially converted into the compound with the 425 nm band. The concomitant changes in the IR-spectrum also testify to that transformation (Fig. 8, dashed spectrum). The reverse transformation can be achieved by 1 h irradiation at 365 nm (Fig. 8, solid spectrum). This latter photolysis leads, however, to the concomitant bleaching of some azide **1** which had not been decomposed during the initial 254 nm photolysis, and therefore to the formation of some nitrene **4**. We will show, with the help of the quantum chemical calculations described in the next section, that our original assignment of the two intermediates had indeed been correct.

Quantum chemical calculations of the properties of nitroso oxides

Quantum chemical calculations of the IR- and UV-spectra of the nitroso oxides **7** and **8** were performed to assign the experimental spectral data. It has been argued[8,38–41] that the ground states of nitroso oxides have substantial diradical character, similar to ozone. In view of this, the geometries of **7** and **8** were not only optimized by the restricted and unrestricted B3LYP, but also by the CASSCF method.

According to RB3LYP/6-31G(d) the singlet ground states of *cis*- and *trans*-nitroso oxides **7** and **8** are planar, apart from the slightly pyramidal amino groups (see Fig. 9). The bond-length pattern indicates the participation of a quinoidal resonance structure (Scheme 3): in addition to significant bondlength alternation in the aromatic ring, the H_2N–C bond is shorter than in aniline (1.400 Å by the same method) and the C–NOO bond is shorter than in Me–NOO (where it is 1.452 Å). This partial double bond character of the C–NOO bond enforces planarity even to the *cis*-isomer, in spite of the sterically unfavorable interaction of the terminal O atom with

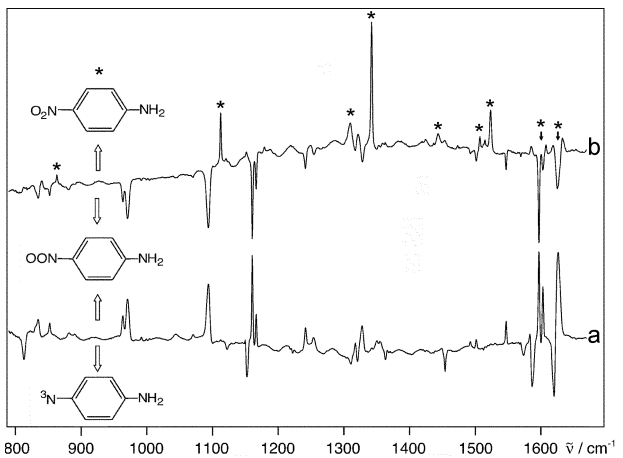

Fig. 5 Difference IR spectrum for the annealing of nitrene **4** in an Ar matrix containing 4% oxygen at 30 K (spectrum *a*) and changes upon subsequent 5 min irradiation at >515 nm (spectrum *b*). The asterisks mark the positions of experimental IR peaks of *p*-nitroaniline (**2**) in an Ar matrix at 12 K.

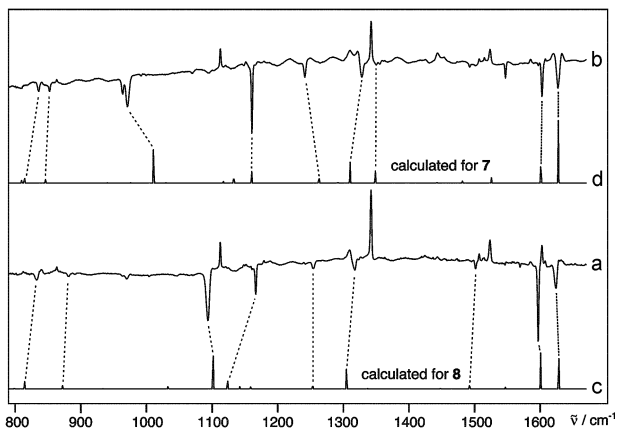

Fig. 7 Difference IR spectra produced by bleaching of the adducts of nitrene **4** with oxygen in an Ar matrix at >515 nm for 30 s (spectrum *a*) and 5 min (spectrum *b*). The traces *c* and *d* show the IR spectra of *trans*- (**8**) and *cis*- (**7**) *p*-aminophenylnitroso oxides, respectively, calculated by B3LYP and scaled by 0.9614.

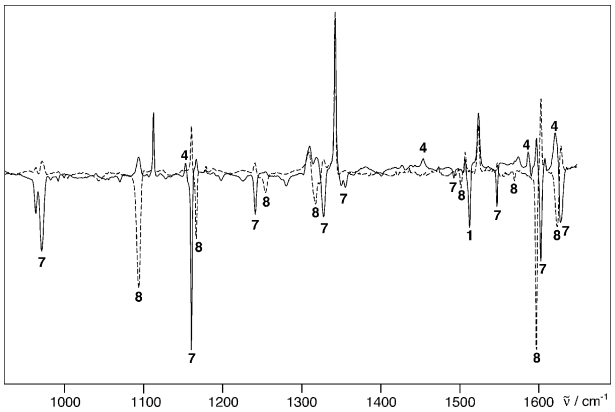

Fig. 8 Changes in the IR spectra of the mixture of nitroso oxides **7** and **8** upon 30 min irradiation at 515 nm (dashed difference spectrum) and subsequent 365 nm photolysis during 60 min (solid difference spectrum) through a monochromator. The IR-bands of compounds **1**, **4**, **7** and **8** are indicated by the corresponding numbers.

the nearest H-atom in the aromatic ring which causes an opening of the C–C–N angle to 131° (the rotational barrier for the NOO group amounts to 14 kcal mol^{-1}).

The calculated IR spectra of the two isomers, **7** and **8**, are presented in Fig. 7 as traces *d* and *c*, respectively. Although quantitative agreement is not optimal (perhaps due to an inadequacy of the RDFT method to treat these species), the pattern of downward pointing peaks in spectrum *a* coincides better with those calculated for the *trans*-isomer **8** (trace *c*), whereas the same peaks in trace *b* correlate better with those calculated for the *cis*-isomer **7** (trace *d*). In particular, our assignment rests on the occurrence of a strong peak (split into two components, presumably due to a site effect) at *ca.* 970 cm^{-1} for **7**, whereas **8** (for which no IR bands are predicted in that region) has a strong peak at 1090 cm^{-1}, in good accord with the B3LYP prediction. From a comparison of the concomitant spectral changes in the IR and UV-Vis regions we

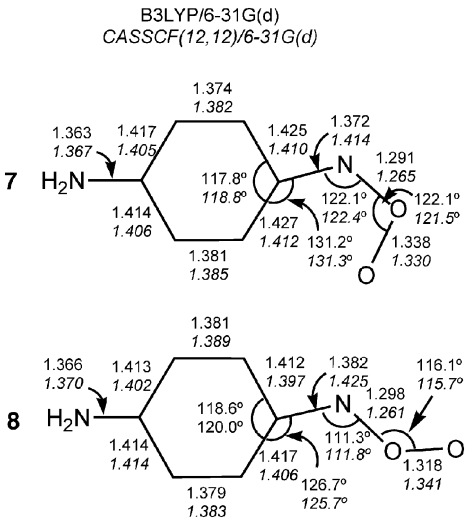

Fig. 9 Bond lengths (Å) and bond angles in the ground states of the *cis*- and *trans*-isomers of *p*-aminophenylnitroso oxide calculated by B3LYP (normal font) and CASSCF(12,12) methods (italic).

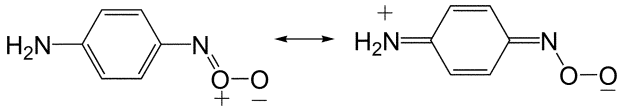

Scheme 3

conclude that the absorbance maximum at 460 nm must be attributed to **8**, whereas **7** is responsible for the band peaking at 425 nm.

However, we found that the restricted singlet ground state wavefunction of the *trans*-isomer **8** is unstable (in contrast to that of the *cis*-isomer **7** which is stable): an unrestricted B3LYP calculation[42] of **8** leads to a lowering of the electronic energy by 1.7 kcal mol^{-1} accompanied by a triplet contamination of the wavefunction ($\langle S^2 \rangle$ = 0.475, 0.034 after annihilation of the triplet component). Geometry optimization by the UB3LYP procedure resulted in a significant lengthening of the N–O bond (1.339 *vs.* 1.298 Å by RB3LYP). In spite of this, the IR spectra of **8** calculated by UB3LYP and RB3LYP are very similar (*cf.* ESI, Fig. S3),† with the latter actually being in slightly better agreement with experiment.

In order to simplify the CASSCF calculations, we constrained the amino groups of **7** and **8** to be coplanar with the phenyl rings (B3LYP calculations had shown that the energy difference between the planar and the slightly twisted equilibrium structures of **7** and **8** is very small—0.13 kcal mol^{-1} and 0.24 kcal mol^{-1}, respectively—and that flattening the NH_2 group does not affect the geometry of the Ph-NOO moiety). The active space used in the CASSCF calculations comprised two σ-, and four π-MOs containing 12 electrons in addition to two σ*- and four π* virtual MOs.

The structures of planar **7** and **8** calculated by the B3LYP and CASSCF(12,12) methods are shown in Fig. 9 from which it can be gathered that the lengths of NO–, OO– and CN-bonds of **7** and **8** differ appreciably (0.02–0.04 Å) between the two methods, although both agree in predicting a slightly quinoid geometry (see above). Both methods predict the length of the NO-bond to be close to that of a double bond, while the O–O bond-length is closer to that of a single bond, in agreement with the dominant resonance structure (Scheme 3).

The following configurations make the largest contributions to the wave function of the singlet ground state of **7**: 82.7% ground configuration, 2.5% doubly excited HOMO → LUMO and 1.7% doubly excited (HOMO − 1) → (LUMO + 1). In **8** the corresponding contributions are 82.0, 2.5 and 1.8 %, respectively. As the CASSCF natural orbital occupation numbers showed no significant deviation from 0 or 2 (at most 0.13 for the HOMO and the LUMO) we conclude that the CASSCF calculations do not lend support to the claim[8,38–41] that the ground states of nitroso oxides have a high diradical character.

To gauge whether the geometries of the nitroso oxides calculated by B3LYP or CASSCF are closer to the real structure, we calculated the vertical excitation energies and oscillator strengths of **7** and **8** by the CASSCF(16,14)/CASPT2 method[43] at the B3LYP and CASSCF (12,12) geometries (Tables 2 and 3 and bar graphs in Figs. 6 and 10). The position of the most intense transition, $1\ ^1A' \rightarrow 2\ ^1A'$ was

Table 2 Vertical excitation energies of *cis-p*-aminophenylnitroso oxide **7** calculated by the CASPT2 method[a]

State	ΔE_{CASSCF}/eV	ΔE_{CASPT2}/eV	Reference weight[b]	λ/nm	f[c]	Major configurations[d]
$1\ ^1A'$	0.00	0.00	0.73	—	—	69% ground config. −3% 6a″ → 7a″
$1\ ^1A''$	2.83	2.47	0.69	502	1.2×10^{-6}	83% 30a′ → 7a″
$2\ ^1A'$	4.62	3.00	0.71	413	3.0×10^{-1}	54% 6a″ → 7a″ + 7% ground config.
$3\ ^1A'$	3.95	3.81	0.72	326	3.5×10^{-3}	22% 6a″ → 8a″ + 13% 5a″ → 7a″ + 12% 4a″ → 7a″
$4\ ^1A'$	4.00	3.89	0.72	319	2.1×10^{-2}	21% 2(6a″ → 7a″) +14% 4a″ → 7a″
$5\ ^1A'$	5.84	4.83	0.71	257	9.0×10^{-3}	20%: 5a″ → 7a″ + 14%: 6a″ → 8a″
$6\ ^1A'$	6.19	4.96	0.69	250	3.9×10^{-2}	24%: 4a″ → 8a″

[a] Based on a CASSCF(16,14)/ANO-S wave function at the CASSCF(12,12)/6-31G(d) geometry; The A″ state was calculated with no level shift, A′ states with a level shift of 0.2 h. [b] Weight of the zero-order CASSCF in the CASPT2 wave function. [c] Oscillator strength for electronic transition. [d] Electron excitations within the active space of orbitals depicted in Fig. 10.

found to coincide much better with the experimental spectra when it was calculated at the CASSCF than at the B3LYP geometries of **7** and **8** (see ESI, Tables S5 and S8).† From this we conclude that the geometries of the two isomeric nitroso oxides optimized by CASSCF are closer to the real ones.

In contrast, the positions of the $1\ ^1A' \rightarrow 2\ ^1A'$ transition calculated by the TD-B3LYP/6-311+G(d) method were found to depend only slightly on the geometry (for **7** λ_{max} = 351 nm at the CASSCF and 356 nm at the B3LYP structure; for **8** the corresponding values are λ_{max} = 395 and 398 nm, respectively). However, agreement between theory and experiment is much less satisfactory, so we cannot use the excitation energies calculated by the TD-DFT method to assess the quality of the geometries of **7** and **8** calculated by B3LYP or CASSCF.

As mentioned above, Brinen and Singh had reported the formation of both diamagnetic and paramagnetic products upon photolysis of the 1,4-diazidobenzene in a glassy matrix.[6] Although this finding could not be reproduced in subsequent studies, [3,5,7,8] the Wigner selection rules do not prohibit in principle two triplet reactants from forming triplet products. Thus we decided to perform calculations of the thermodynamics of the formation of adducts between triplet nitrene and molecular oxygen and their further rearrangements in both spin states by the B3LYP/6-311G(d,p), the G2M(CC5)[26] and the CBS-QB3[25] level of theory (see ESI, Figs. S4–S5 and Tables S10–S12 for complete results).†

The results from the CBS-QB3 calculations, which have proven to be quite reliable in a recent study of the reaction of phenylnitrene with oxygen,[44] are summarized in Fig. 11 which shows that the reactions of ^{3}**4** with $^3O_2$ to form the singlet adducts **7** or **8** are strongly exothermic. Moreover, substituents

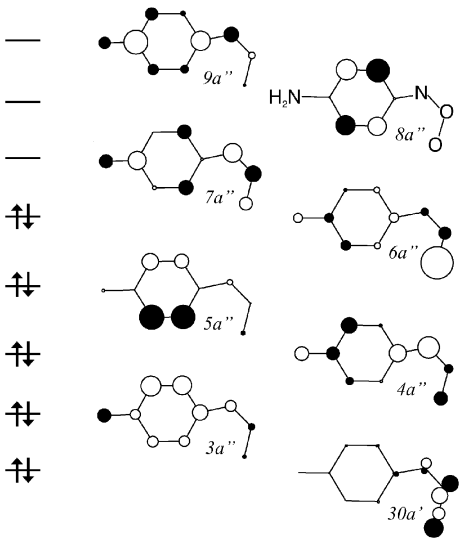

Fig. 10 MOs involved in the electronic transitions of the nitroso oxides **7** and **8**, shown on the example of **7** (*cf.* Table 2 and 3)

do not have a large influence on the reaction enthalpy which is in the range of 18.5 to 20 kcal mol^{-1} for *cis*- and *trans*-isomers of phenyl- and *para*-aminophenylnitroso oxides. The value of the singlet–triplet splitting in **7** and **8** is also practically independent of the substitution and is equal to 15.5–18 kcal mol^{-1}. As a consequence, the formation of the products in their triplet excited states is almost thermoneutral. However, if the nitroso oxides were formed in their triplet states they would very quickly convert to their singlet ground states.

Table 3 Vertical excitation energies of *trans-p*-aminophenylnitroso oxide **8** calculated by the CASPT2 method[a]

State	ΔE_{CASSCF}/eV	ΔE_{CASPT2}/eV	Reference weight[b]	λ/nm	f[c]	Major configurations[d]
$1\ ^1A'$	0.00	0.00	0.71			63% ground config. −10% 6a″ →7a″
$1\ ^1A''$	1.88	2.42	0.69	511	8.9×10^{-6}	84%: 30a′ → 7a″
$2\ ^1A'$	4.38	2.77	0.69	448	4.5×10^{-1}	49% 6a″ → 7a″ + 15% ground config.
$3\ ^1A'$	3.80	3.48	0.70	357	2.9×10^{-2}	29% 6a″ → 8a″
$4\ ^1A'$	3.70	3.61	0.70	343	1.0×10^{-2}	19% 2(6a″→7a″) + 15% 6a″ →9a″ + 11% 4a″ → 7a″
$5\ ^1A'$	5.86	4.99	0.70	249	3.0×10^{-3}	14% 4a″ →8a″ + 11% (6a″ →7a″ + 6a″ → 8a″)
$6\ ^1A'$	5.62	5.08	0.68	244	2.1×10^{-3}	12% (6a″ →7a″ +5a″ → 8a″) + 11% (6a″ → 7a″ + 4a″ → 8a″)

[a] Based on a CASSCF(16,14)/ANO-S wave function at the CASSCF(12,12)/6-31G(d) geometry; A″ state was calculated with no level shift, A′ states with a level shift of 0.15 h. [b] See footnotes to Table 2. [c] See footnotes to Table 2. [d] Electron excitations within the active space of orbitals which are similar to those of **7** depicted in Fig. 10.

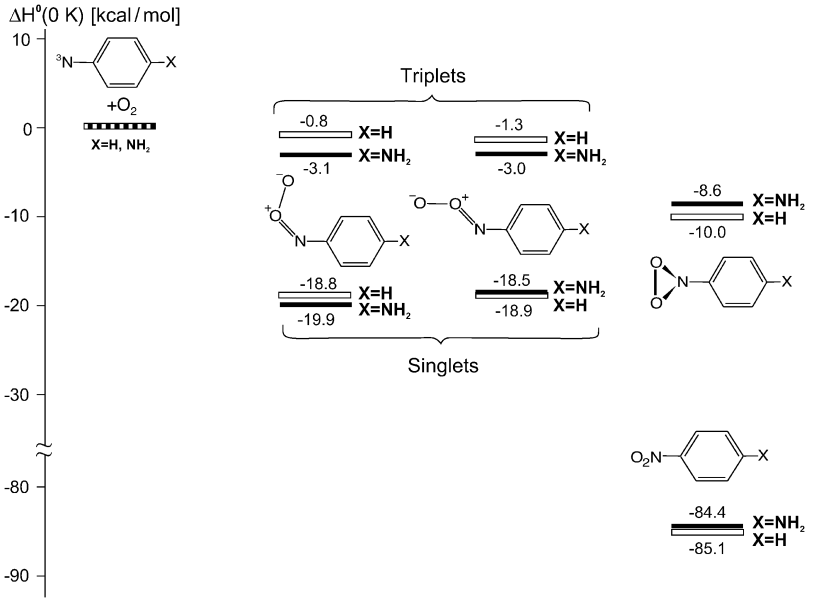

Fig. 11 Relative 0 K enthalpies of the species involved in the formation and rearrangement of phenyl- (open bars) and *p*-aminophenylnitroso oxides (solid bars) calculated by the CBS-QB3 method.

Therefore, the triplet species detected in the early study of Brinen and Singh[6] cannot be assigned to a nitroso oxide with an aryliminodiradical structure.

Photobleaching of the nitroso oxides **7** and **8** leads to *p*-nitroaniline **2** (*cf*. Fig. 4 and 5). It has been proposed[6] that the photochemical formation of nitro compounds from nitroso oxides proceeds *via* intermediate dioxaziridines (Scheme 4). Formation of such compounds on high intensity photolysis of nitroso oxides was observed in glassy matrices at 77 K by Harder *et al*. using UV-Vis spectroscopy.[8]

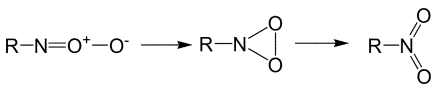

Scheme 4

We were unable to reproduce this experiment in argon matrices at 12 K irrespective of the source and intensity of the light we used. Fig. 11 shows that rearrangements of nitroso oxides **7** and **8** to dioxaziridine **9** are endothermic reactions with an enthalpy change of about 11 kcal mol^{-1} at 0 K. This precludes of course only thermal, but not photochemical isomerization of **7** and **8** to **9**. However, no IR bands of dioxaziridine **9** were detected on irradiation of **7** and **8** by a Xe lamp through glass filters or a monochromator. Calculated IR and EA spectra of the cyclic dioxaziridine are presented in the ESI (Fig. S6 and Table S13).†

4 Conclusion

We have studied the photochemical transformations of **1** in argon matrices in the absence and presence of oxygen. Thereby, and with the help of quantum chemical calculations we were able to characterize the triplet nitrene **4** as well as the *cis*- and *trans*-nitroso oxides **7** and **8**. We found that the latter two isomers can be interconverted by irradiation at selected wave lengths and that they are ultimately converted into *p*-nitroaniline **2**. Although restricted wave functions of the nitroso oxides are unstable, CASSCF calculations turned up no evidence for the claimed diradical character of these compounds. Also we found no evidence for triplet products resulting from the reaction of **4** with oxygen, nor for dioxaziridines as intermediates of the conversion of the nitroso oxides to **2**. Our findings are summarized in Scheme 5.

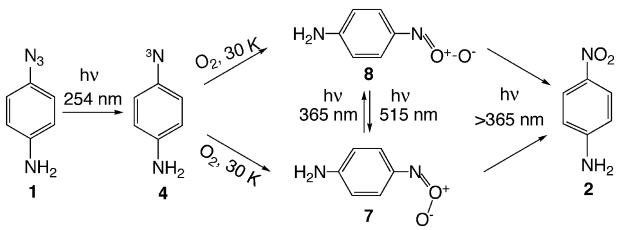

Scheme 5

Acknowledgements

The authors are grateful to the Ministry of Science and Education of the Russian Federation (grant N E02-5.0-27), Division of Chemistry and Material Sciences of the Russian Academy of Sciences and the Swiss National Science Foundation (project No 200020-105217 and SCOPES grant No 7SUPJ062336).

References

1 W. T. Borden, N. P. Gritsan, C. M. Hadad, W. L. Karney, C. R. Kemnitz and M. S. Platz, *Acc. Chem. Res.*, 2000, **33**, 765.
2 N. P. Gritsan and M. S. Platz, *Adv. Phys. Org. Chem.*, 2001, **36**, 255.
3 N. P. Gritsan and E. A. Pritchina, *Russ. Chem. Rev.*, 1992, **61**, 500.
4 Y.-Z. Li, J. P. Kirby, M. W. George, M. Poliakoff and G. B. Schuster, *J. Am. Chem. Soc.*, 1988, **110**, 8092.
5 E. A. Pritchina and N. P. Gritsan, *J. Photochem. Photobiol., A: Chem.*, 1988, **43**, 165.
6 J. S. Brinen and B. Singh, *J. Am. Chem. Soc.*, 1971, **93**, 6623.
7 N. P. Gritsan and E. A. Pritchina, *J. Inf. Rec. Mater.*, 1989, **178**, 391.
8 T. Harder, P. Wessig, J. Bendig and R. Stosser, *J. Am. Chem. Soc.*, 1999, **121**, 6580.
9 E. M. Chainikova, S. L. Hursan and R. L. Safiulllin, *Proc. Russ. Acad. Sci*, 2004, **396**, 793 (in Russian).
10 Formation of both singlet and triplet states of the same intermediate looks surprising. However, there is a precedent in the literature: both singlet and triplet states of 2-naphthyl-(carbomethoxy)carbene were detected in an Ar matrix due to a pronounced difference in conformation of these states. See: Z. Zhu, T. Bally, L. L. Stracener and R. J. McMahon, *J. Am. Chem. Soc.*, 1999, **121**, 2863.
11 S. V. Zelentsov, E. B. Kormiltseva and A. B. Zhezlov, *Khim. Vys. Energ.*, 2002, **50**, 122 (in Russian).
12 P. A. S. Smith, J. R. Hall and R. O. Kan, *J. Am. Chem. Soc.*, 1962, **84**, 485.
13 T. Bally, in *Reactive Intermediate Chemistry*, ed. R. A. Moss, M. A. Platz and M. Jones, New York, 2004, p. 797.
14 A. D. Becke, *J. Chem. Phys.*, 1993, **98**, 5648.
15 C. Lee, W. Yang and R. G. Parr, *Phys. Rev. B*, 1988, **37**, 785.
16 B. O. Roos, *Adv. Chem. Phys.*, 1987, **69**, 399.
17 M. J. Frisch, G. W. Trucks, H. B. Schlegel, G. E. Scuseria, M. A. Robb, J. R. Cheese, V. G. Zakrzewski, J. A. Montgomery, R. E. Stratmann, J. C. Burant, S. Dapprich, J. M. Millam, A. D. Daniels, K. N. Kudin, M. C. Strain, O. Farkas, J. Tomasi, V. Barone, M. Cossi, R. Cammi, B. Mennucci, C. Pommelli, C. Adamo, S. Clifford, J. Ochterski, G. A. Petersson, P. Y. Ayala, Q. Cui, K. Morokuma, D. K. Malick, A. D. Rabuck, K. Raghavachari, J. B. Foresman, J. Cioslowski, J. V. Ortiz, B. B. Stefanov, G. Liu, A. Liashenko, P. Piskorz, I. Komaromi, R. Gomperts, R. L. Martin, D. J. Fox, T. Keith, M. A. Al-Laham, C. Y. Peng, A. Nanayakkara, M. Challacombe, P. M. W. Gill, B. G. Johnson, W. Chen, M. W. Wong, J. L. Andres, C. Gonzales, M. Head-Gordon, E. S. Repogle and J. A. Pople, in *GAUSSIAN 98*, Pittsburgh PA, 1998.
18 K. Andersson, M. R. A. Blomberg, M.P. Fülscher, V. Kellö, R. Lindh, P.-Å. Malmqvist, J. Noga, J. Olson, B. O. Roos, A. Sadlej, P. E. M. Siegbahn, M. Urban and P.-O. Widmark, in *MOLCAS*, 1994.
19 A. P. Scott and L. Radom, *J. Phys. Chem.*, 1996, **100**, 16502.
20 K. Andersson and B. O. Roos, in *Modern Electronic Structure Theory, Part 1, Volume 2*, Singapore, 1995.
21 K. Pierloot, B. Dumez, P.-O. Widmark and B. O. Roos, *Theor. Chim. Acta*, 1995, **90**, 87.
22 B. O. Roos, K. Andersson, M. P. Fülscher, L. Serrano-Andrés, K. Pierloot, M. Merchan and V. Molina, *J. Mol. Struct. (THEOCHEM)*, 1996, **388**, 257.
23 M. E. Casida, in *Recent Advances in Density Functional Methods, Part 1*, ed. D. P. Chong, World Scientific Publishers, Singapore, 1995, p. 150.
24 K. B. Wiberg, R. E. Stratmann and M. J. Frisch, *Chem. Phys. Lett.*, 1998, **297**, 60.
25 J. A. Montgomery, M. J. Frisch and J. Ochterski, *J. Chem. Phys.*, 1999, **110**, 2822.
26 A. M. Mebel, K. Morokuma and M. C. Lin, *J. Chem. Phys.*, 1995, **103**, 7414.
27 G. C. Eiden and J. C. Weisshaar, *J. Chem. Phys.*, 1996, **104**, 8896.
28 S. Matzinger and T. Bally, *J. Phys. Chem. A*, 2000, **104**, 3544.
29 I. R. Dunkin and P. C. P. Thomson, *J. Chem. Soc., Chem. Commun.*, 1980, 499.
30 J. Morawietz and W. Sander, *J. Org. Chem.*, 1996, **61**, 4351.
31 O. L. Chapman and J.-P. LeRoux, *J. Am. Chem. Soc.*, 1978, **100**, 282.
32 J. C. Hayes and R. S. Sheridan, *J. Am. Chem. Soc.*, 1990, **112**, 5879.
33 N. P. Gritsan, Z. Zhu, C. M. Hadad and M. S. Platz, *J. Am. Chem. Soc.*, 1999, **121**, 1202.
34 According to TD-B3LYP/6-31+G(d) calculations keteneimine **5** has a UV-spectrum with maxima at 401 nm ($f = 1.2 \times 10^{-2}$) and 353 nm ($f = 3.2 \times 10^{-2}$).
35 These two transition derive from the degenerate excitation at 3.65 eV ($f = 1.8 \times 10^{-2}$) of the simplest nitrene, ^{3}NH, which originates from electron promotion of the N sp-lone pair to the degenerate singly occupied p-AOs.
36 In the region 600–1700 cm^{-1}: 832.5, 881, 1093.5, 1166.5, 1254, 1317.5, 1501.5, 1569, 1597, 1624 cm^{-1}.
37 In the region 600–1700 cm^{-1}: 836, 852.5, 963.5 + 971, 1070, 1094.5, 1160.5, 1241.5, 1350 + 1355, 1492.5, 1547, 1602.5, 1627 cm^{-1}.
38 T. Fueno, K. Yokoyama and S. Takane, *Theor. Chim. Acta*, 1992, **82**, 299.
39 S. L. Laursen, J. E. Grace, R. L. DeKock and S. A. Spronk, *J. Am. Chem. Soc.*, 1998, **120**, 12583.
40 P. Ling, A. I. Boldyrev, J. Simons and C. A. Wright, *J. Am. Chem. Soc.*, 1998, **120**, 12327.
41 S. Ishikava, S. Tsuji and Y. Sawaki, *J. Am. Chem. Soc.*, 1991, **113**, 4282.
42 M. H. Lim, S. E. Worthington, F. J. Dulles and C. J. Cramer, in *Density Functional Methods in Chemistry (ACS Symposium Series, Vol 29)*, ed. B. B. Laird, R. B. Ross and T. Ziegler, American Chemical Society, Washington, DC, 1996, p. 402.
43 Problems with intruder states in the CASPT2 calculations made it necessary to add two lower-lying π orbitals to the active space.
44 J. Liu, C. M. Hadad and M. S. Platz, *Org. Lett.*, 2005, **7**, 549.